Electronic Supplementary Material (ESI) for Dalton Transactions

Keggin polyanions and copper clusters based coordination polymer towards model for complex nanosystem

Supporting Information

Materials and general methods. All chemicals were commercially purchased and used as supplied. Elemental analyses of C, H, and N were performed using an EA1110 elemental analyzer. The IR spectrum was recorded in the range 4000-400cm^{-1} on a Nicolet 360 spectrometer with a pressed KBr pellet. The TG-DTA analysis was carried out by Universal Analysis 2000 thermogravimetric analyzer (TGA) in N_2 with a heating rate of 10 °C /min. The powder X-ray diffraction (PXRD) data was collected on a X'Pert-ProMPD (Holand) D/max-γA X-ray diffractometer with Cu Kα radiation in a flat plate geometry. Crystal data were collected on a Bruker X8 APEX II-CCD single crystal X-ray diffractometer with Cu Kα radiation (λ = 0.71073Å).

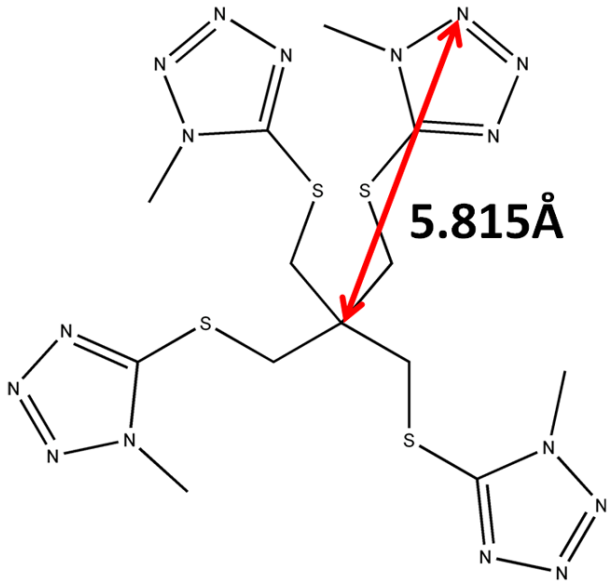

Scheme S1. The bpbb ligand used in this report.

Table S1. Crystal Data and Structural Refinements for FUNSOM-1 and FUNSOM-2.

	FUNSOM-1	FUNSOM-2
formula	$C_{26}Cu_4S_8N_{32}H_{40}PMo_{12}O_{40}Cl$	$C_{26}Cu_4S_8N_{32}H_{44}SiMo_{12}O_{44}$
*F*w	3169.24	3198.94
crystal system	tetragonal	tetragonal
space group	P4nc	I-42d
a (Å)	14.6513(5)	20.3235(14)
b (Å)	14.6513(5)	20.3235(14)
c (Å)	19.1456(15)	39.008(6)
α (deg)	90	90
β (deg)	90	90
γ (deg)	90	90

V (Å^3)	4109.8(4)	16112(3)
Z	2	8
*D*c (g/cm^3)	2.561	2.637
μ (mm^{-1})	3.130	3.161
F(000)	3040.0	12304.0
collcd reflns	14153	28928
unique reflns	3601	6894
obsd reflns	3222	6804
no. of param	293	594
R_{int}	0.027	0.0304
GOF	1.308	1.155
R1[a] [I >2σ(I)]	0.046	0.099
wR2[b](all data)	0.1249	0.2164

[a]$R1 = \sum||F_o|-|F_c||/\sum|F_o|$; [b]$wR2 = \sum[w(F_o^2-F_c^2)^2]/\sum[w(F_o^2)^2]^{1/2}$.

Table S2. Selected bond distances (Å) and angles (°) for FUNSOM-1 and FUNSOM-2.

FUNSOM-1			
Cu(1)-N(1)	1.988(8)	Cl(1)-Cu(1)#2	2.4752(13)
Cu(1)-N(5)	2.018(7)	Cl(1)-Cu(1)#3	2.4752(13)
Cu(1)-N(6)#2	2.072(8)	Cl(1)-Cu(1)#1	2.4752(13)
Cu(1)-Cl(1)	2.4752(13)		
N(1)-Cu(1)-N(5)	124.0(3)	N(1)-Cu(1)-Cl(1)	103.4(3)
N(1)-Cu(1)-N(6)#2	115.3(3)	N(5)-Cu(1)-Cl(1)	100.9(2)
N(5)-Cu(1)-N(6)#2	111.0(3)	N(6)#2-Cu(1)-Cl(1)	96.3(2)
FUNSOM-2			
Cu(1)-N(5)	1.986(17)	Cu(2)-N(13)	1.932(18)
Cu(1)-N(1)	2.005(18)	Cu(2)-N(9)	1.96(2)
Cu(1)-N(6)#1	2.103(17)	Cu(2)-N(2)	2.064(19)
Cu(1)-O(1W)	2.378(17)	Cu(2)-O(1W)	2.288(16)
N(5)-Cu(1)-N(1)	131.8(7)	N(13)-Cu(2)-N(9)	129.6(9)
N(5)-Cu(1)-N(6)#1	97.5(7)	N(13)-Cu(2)-N(2)	114.4(8)
N(1)-Cu(1)-N(6)#1	127.1(7)	N(9)-Cu(2)-N(2)	113.4(8)
N(5)-Cu(1)-O(1W)	117.9(6)	N(13)-Cu(2)-O(1W)	104.7(7)
N(1)-Cu(1)-O(1W)	87.4(6)	N(9)-Cu(2)-O(1W)	98.2(7)
N(6)#1-Cu(1)-O(1W)	84.1(6)	N(2)-Cu(2)-O(1W)	80.3(6)

Symmetry code: for 1: #1 -y+1, x, z; #2 y, -x+1, z; #3 -x+1, -y+1, z; for 2: #1 -x+1/2, y, -z+7/4.

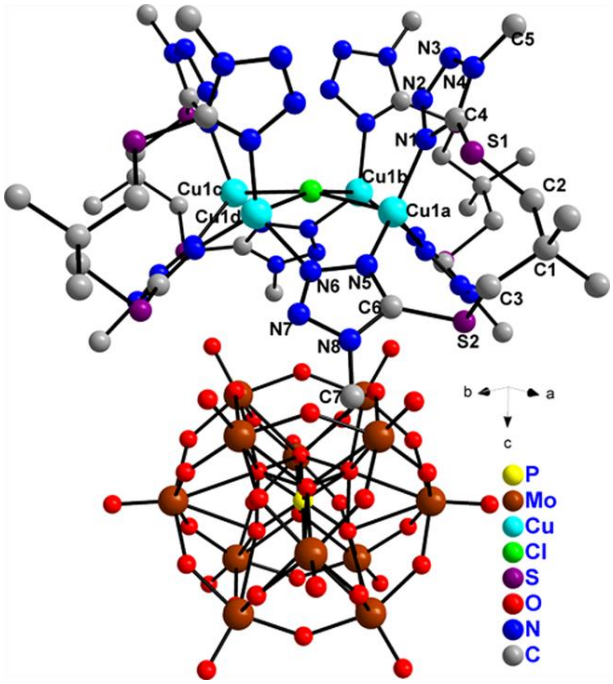

Fig. S1. Ball-stick view of the asymmetric unit of FUNSOM-1. All H atoms are omitted for clarity.

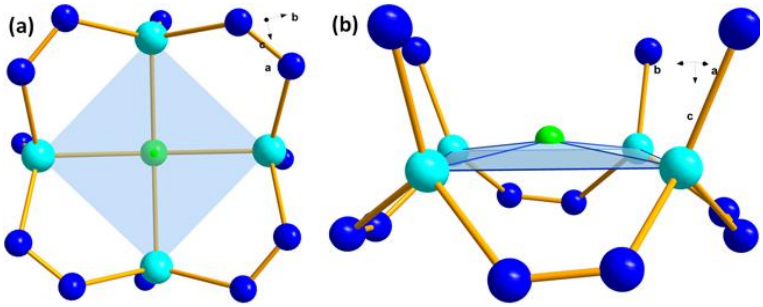

Fig. S2. (a) Top view of the coordination mode of closed Cu_4Cl subunit in FUNSOM-1. (b) The side view of the Cu_4Cl subunit with the centre μ_4-Cl atom residing at the vertex of the tetrahedron.

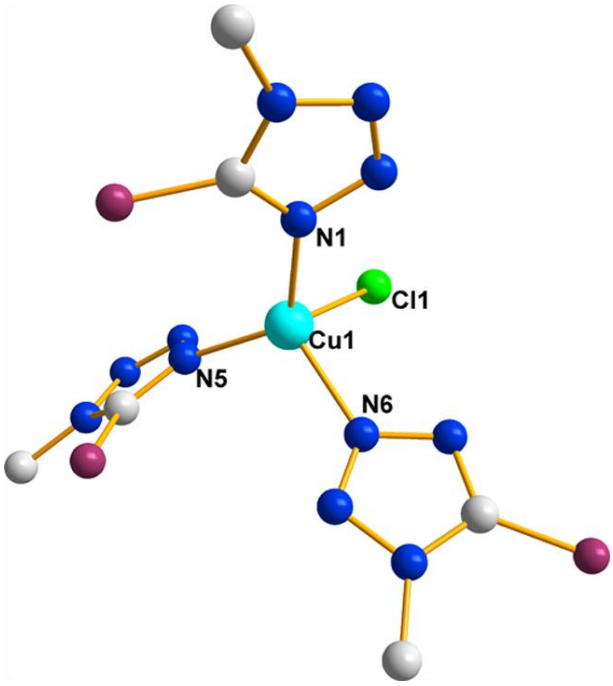

Fig. S3. The coordination detail of Cu1 in FUNSOM-1.

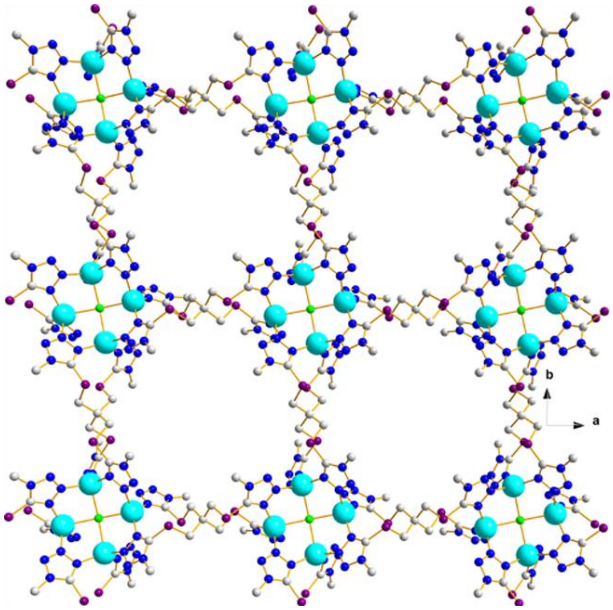

Fig. S4. Details view of the grid-like layer in FUNSOM-1.

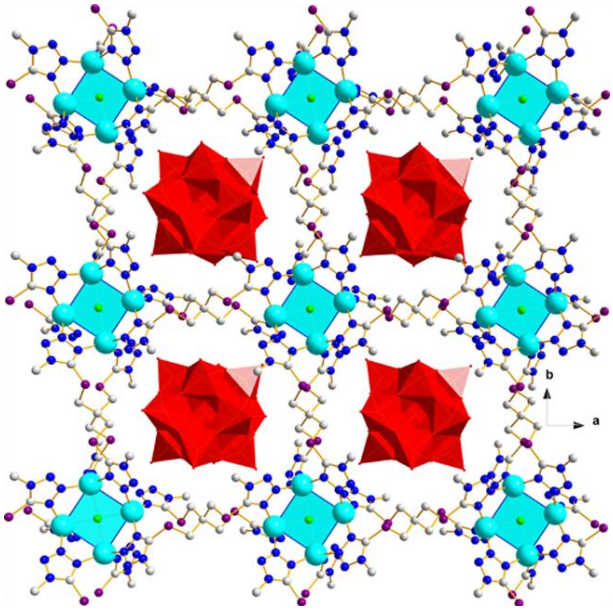

Fig. S5. The relationships between closed $Cu_4Cl(C_2H_3N_4S)_8$ clusters (blue) and $[PMo_{12}O_{40}]^{3-}$ anions (red) in FUNSOM-1.

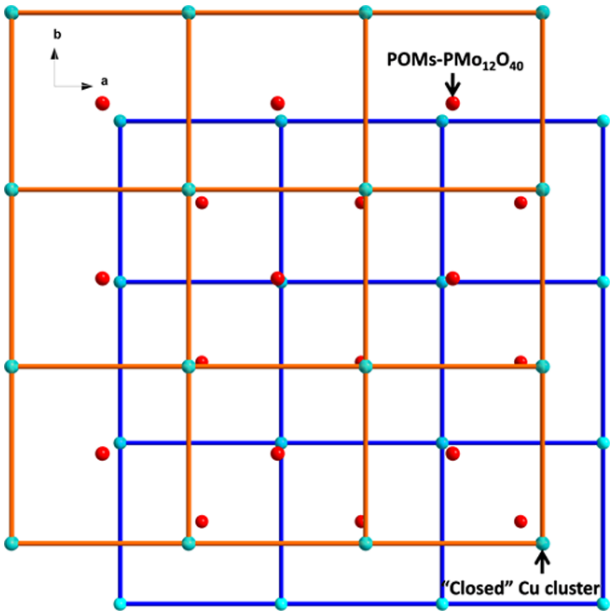

Fig. S6. Two adjacent grid-like layers (blue and yellow) are stagger-packed in FUNSOM-1. The $[PMo_{12}O_{40}]^{3-}$ anions (red) are in the centre of the grids.

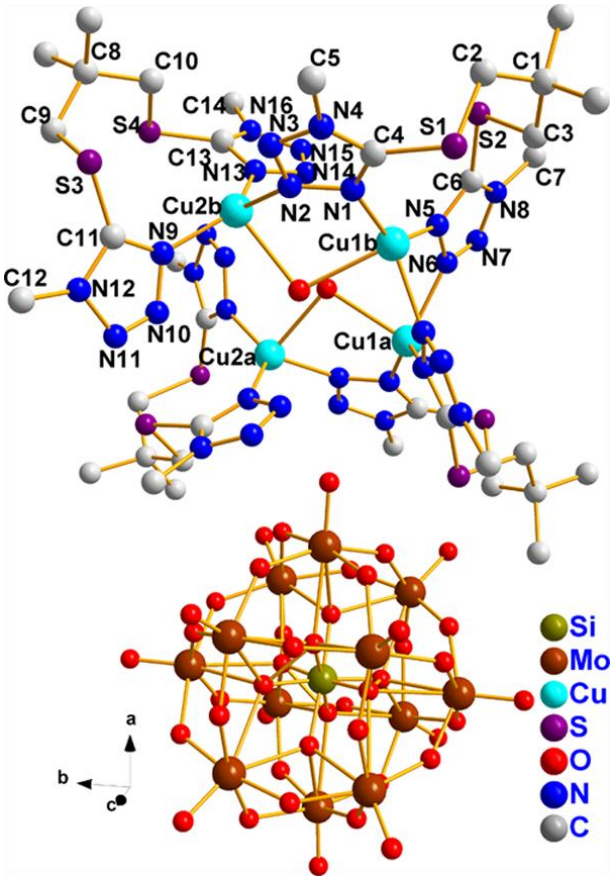

Fig. S7. Ball-stick view of the asymmetric unit of FUNSOM-2. All H atoms are omitted for clarity.

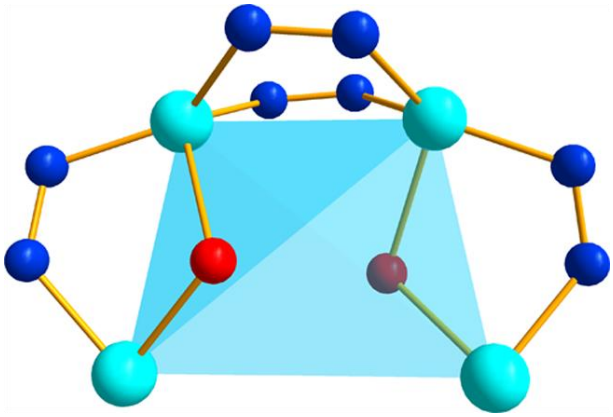

Fig. S8. The coordination mode of open $Cu_4(H_2O)_2$ subunit in FUNSOM-2.

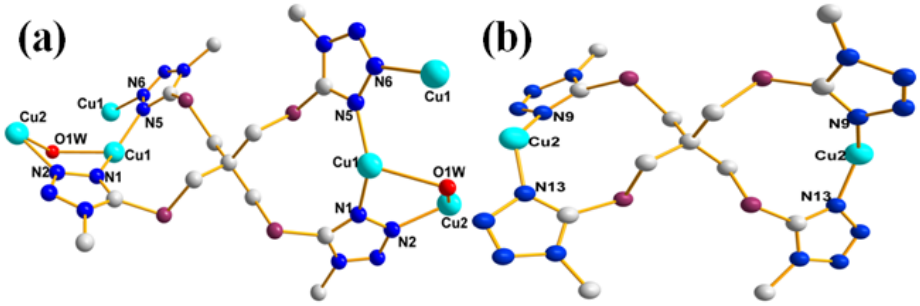

Fig. S9. The multiplex coordination modes of bpbb ligand in FUNSOM-2 (a) bpbb[1] (b) bpbb[2].

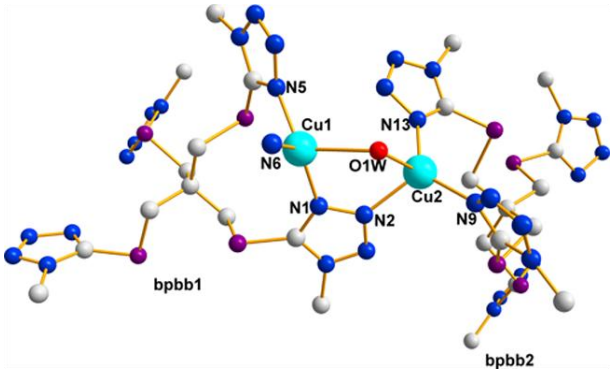

Fig. S10. The coordination details of Cu1 and Cu2 in FUNSOM-2.

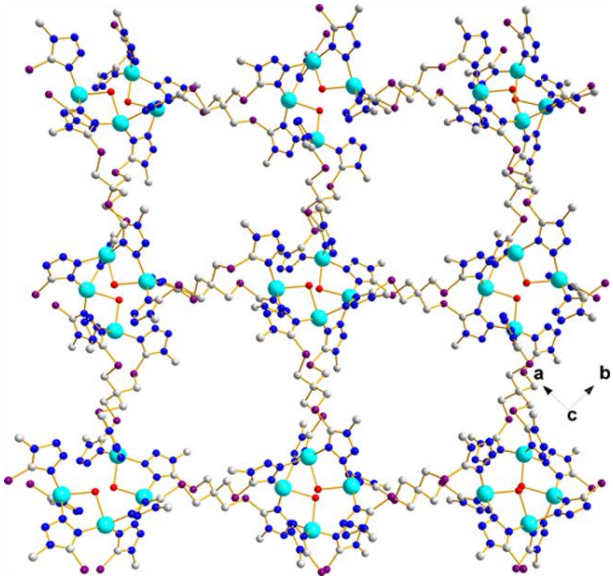

Fig. S11. Details view of the grid-like layer in FUNSOM-2.

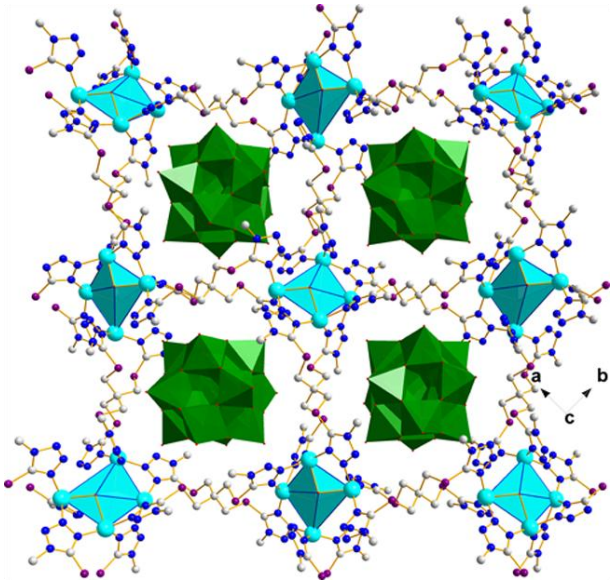

Fig. S12. The relationships between open $Cu_4(H_2O)_2(C_2H_3N_4S)_8$ clusters (blue) and $[SiMo_{12}O_{40}]^{4-}$

anions (green) in FUNSOM-2.

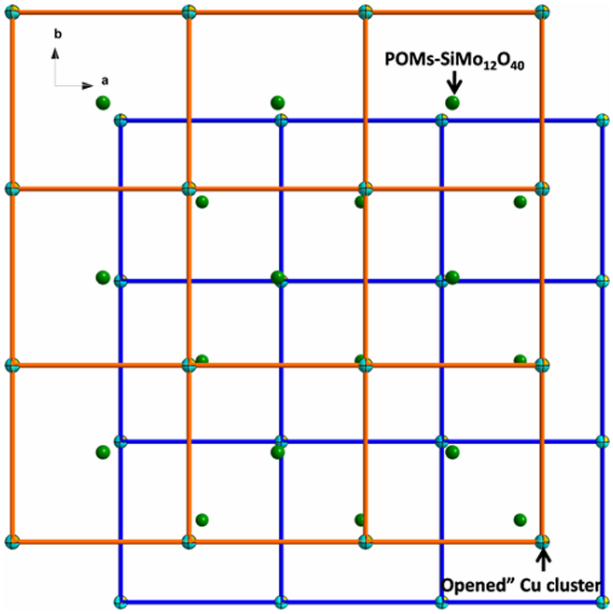

Fig. S13. Two adjacent grid-like layers (blue and yellow) are stagger-packed in FUNSOM-2. The $[SiMo_{12}O_{40}]^{4-}$ anions (green) are in the centre of the grids.

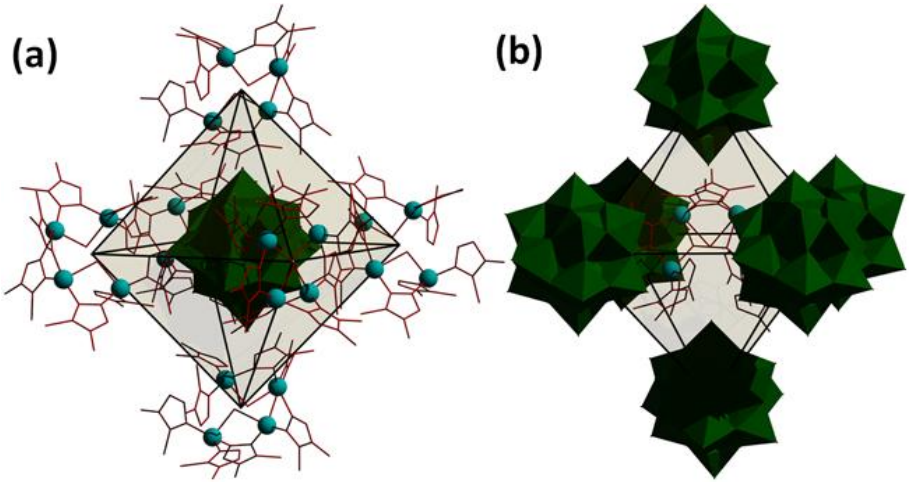

Fig. S14. The arrangement of FUNSOM-2 between $Cu_4(H_2O)_2(C_2H_3N_4S)_8$ nanoclusters and $[SiMo_{12}O_{40}]^{4-}$ anions: (a) one $[SiMo_{12}O_{40}]^{4-}$ anion is surrounded by six $Cu_4(H_2O)_2(C_2H_3N_4S)_8$ nanoclusters; (b) one $Cu_4(H_2O)_2(C_2H_3N_4S)_8$ nanocluster is surrounded by six $[SiMo_{12}O_{40}]^{4-}$ anions.

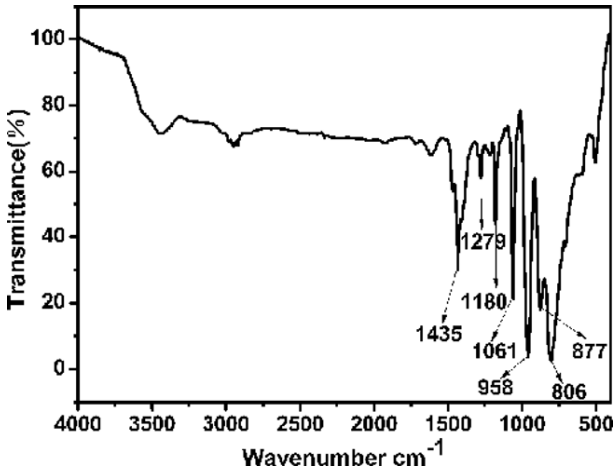

Fig. S15. The IR spectrum of FUNSOM-1 exhibits four characteristic asymmetric vibrations resulting from the $[PMo_{12}O_{40}]^{3-}$ polyanion. The characteristic bands at 806, 877, 958, and 1061 cm^{-1} are attributed to ν(Mo-Ot), ν(Mo-Ob-Mo), ν(Mo-Oc-Mo) and ν(P-O), respectively. The bands in the range of 1171–1618 cm^{-1} are assigned to the vibrations of bpbb ligands.

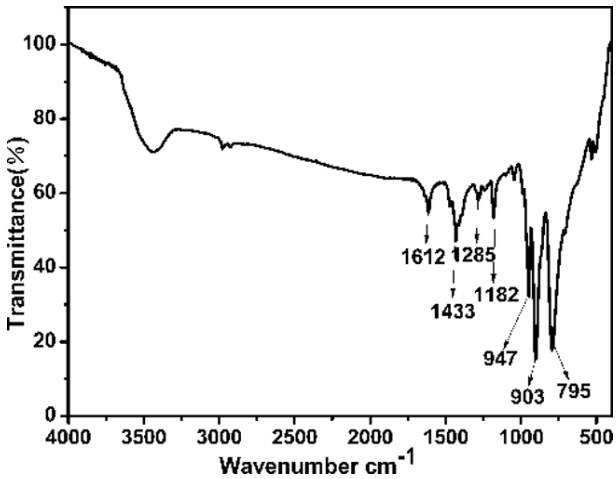

Fig. S16. The IR spectrum of FUNSOM-2 exhibits four characteristic asymmetric vibrations resulting from the $[SiMo_{12}O_{40}]^{4-}$ polyanion. The characteristic bands at 795, 903, and 947 cm^{-1} are attributed to ν(Mo-Ot), ν(Mo-Ob-Mo), ν(Mo-Oc-Mo), and ν(Si-O), respectively. The bands in the range of 1176–1620 cm^{-1} are assigned to the vibrations of bpbb ligands.

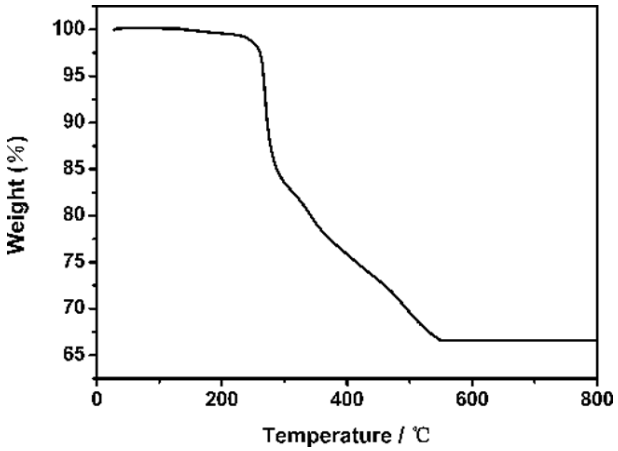

Fig. S17. TG experiments of FUNSOM-1 were performed under N_2 atmosphere with a heating rate of 10 °C/min in the temperature range of 0-1000 ℃. In the TG curves, the weight loss of 33.04% (calc. 33.32%) for FUNSOM-1 from 250 to 550 ℃ corresponds to the loss of bpbb molecules.

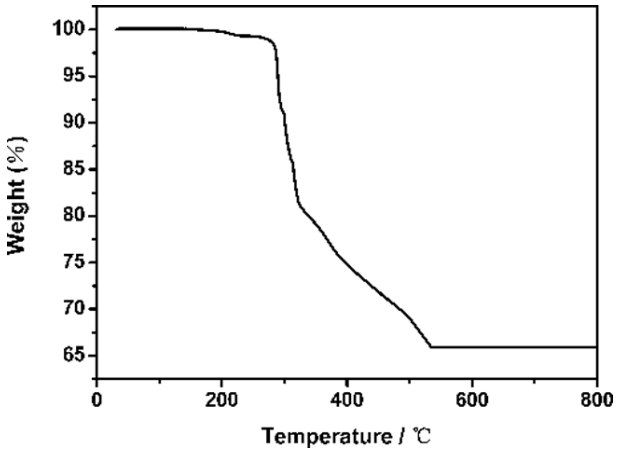

Fig. S18. TG experiments of FUNSOM-2 were performed under N_2 atmosphere with a heating rate of 10 °C/min in the temperature range of 0-1000 ℃. The TG curve indicates that water molecules are eliminated from the network (calcd 0.90%; found 1.13%) when the temperature is increased from room temperature to about 250 °C, after which removal of the organic components (~280 ℃) occurred. The total weight loss was consistent with the calculated values (calcd 34.15%, found 33.98%).

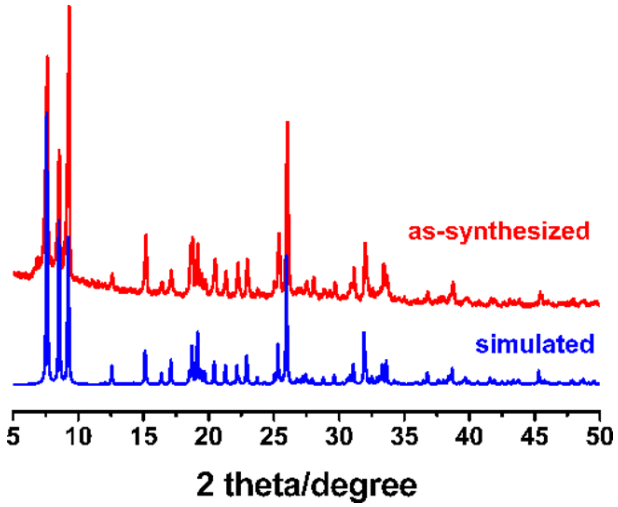

Fig. S19. Experimental XRD patterns of FUNSOM-1 exposed in air (red) and simulation patterns of FUNSOM-1 (blue).

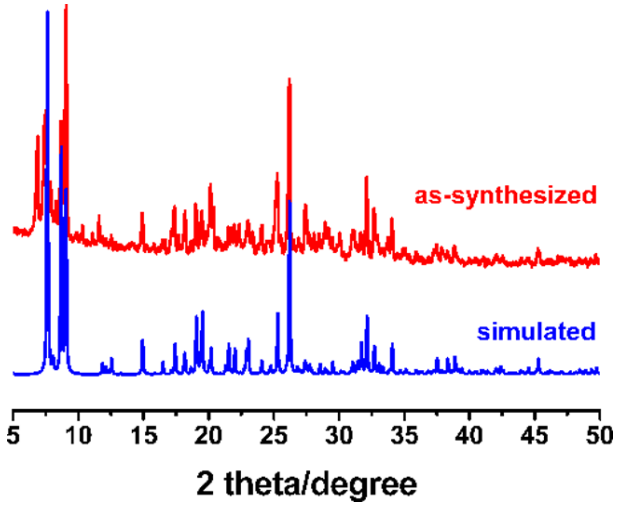

Fig. S20. Experimental XRD patterns of FUNSOM-2 exposed in air (red) and simulation patterns of FUNSOM-2 (blue).